

Effect of Trehalose on Stabilization of Cellular Components and Critical Targets Against Heat Shock in *Saccharomyces cerevisiae* KNU5377

PAIK, SANG-KYOO¹, HAE-SUN YUN¹, HITOSHI IWAHASHI², KAORU OBUCHI², AND INGNYOL JIN^{1*}

¹Department of Microbiology, School of Life Sciences and Biotechnology, Kyungpook National University, Daegu 702-701, Korea

²National Institute of Advanced Industrial Science and Technology, Tsukuba, Ibaraki 305-8566, Japan

Received: January 4, 2005

Accepted: February 7, 2005

Abstract In our previous study [14], we found that heat-shock exposure did not stimulate the neutral trehalase activity in *Saccharomyces cerevisiae* KNU5377, but did in ATCC24858. Consequently, the trehalose content in KNU5377 became 2.6 times higher than that in ATCC24858. Because trehalose has been shown to stabilize the structure and function of some macromolecules, the present work was focused to elucidate the relationship between trehalose content of these strains and thermal stabilities of whole cells, through differential scanning calorimetry (DSC), and to predict critical targets calculated from the hyperthermic cell killing rates. These analyses showed that the prominent DSC transition of both strains gave identical T_m (transition temperature) values in exponentially growing cells, and that the T_m values of critical targets was about 3°C higher in KNU5377 than in ATCC24858. Both heat-shocked KNU5377 and ATCC24858 cells displayed similar shifts in their DSC transition profiles. On the other hand, the T_m value of the critical target of KNU5377 was decreased by 2.1°C, which was still higher than ATCC24858 showing no changes. In view of these results, the intrinsic thermotolerance of KNU5377 did not appear to result from the stability of entire cellular components, but rather possibly from that of particular macromolecules, including critical targets, even though it should be investigated in more details. Although the trehalose levels in heat-shocked cells are significantly different, as described in our previous study [14], the overall pattern of thermal stabilities and their predicted critical targets in two heat-shocked strains seemed to be identical. These data suggest that the trehalose levels examined before and after heat shock of exponentially growing cells are not closely correlated with the stabilities of whole cells and/or critical targets in both yeast strains.

Key words: Thermotolerance, trehalose, DSC, hyperthermic cell-killing kinetics, critical target

The rate constant of hyperthermic cell killing conventionally represents the thermotolerance of living cells. The critical target model, in which thermal damage of particular macromolecules or their complexes is rate limiting for cell killing, relates the tolerance with molecular events. If thermal denaturation rates of some particular molecules or their assemblies determine the cell-killing rate, then they are the critical targets of the hyperthermic cell killing [7, 8]. This model enables us to estimate the Arrhenius parameters of the critical denaturation in *S. cerevisiae* cells [12]. From these parameters, critical denaturation profiles can be predicted as endotherms that could be obtained from differential scanning calorimetry (DSC) [13].

Trehalose has been known to stabilize structures of macromolecules and organelles isolated from *S. cerevisiae* cells [13]. According to the critical target model, if the trehalose accumulation effectively stabilizes the critical targets *in vivo*, then its accumulation confers thermotolerance to the cells [5]. Although other sugars also stabilize macromolecules *in vitro*, none of them are as effective and quantitatively sufficient as trehalose, at least *in vivo*, because this disaccharide occupies an at least 2.5 times larger volume than sucrose, maltose, glucose, and fructose [17]. Wiemken [18] suggested that trehalose accumulation should be critical to acquired thermotolerance in yeast cells after heat shock. On the other hand, Nwaka and Holzer [11] claimed that hydrolysis of trehalose by neutral trehalase should be essential for acquired thermotolerance after heat shock in yeasts. Lepock *et al.* [8], in a series of experiments with *Bacillus* spp., insisted that the maximum growth temperature should be correlated with the stability of cellular components.

In our previous report, a naturally isolated strain *Saccharomyces cerevisiae* KNU5377 exhibited a well-modulated trehalose-related mechanism to accumulate more trehalose by maintaining neutral trehalase activity after heat shock than a reference strain [14]. Therefore, this study was undertaken

*Corresponding author
Phone: 82-53-950-5377; Fax: 82-53-955-5522;
E-mail: jinin@mail.knu.ac.kr

to understand the thermotolerance of *S. cerevisiae* KNU5377 in relation to the stability of cellular components, including predicted critical targets and trehalose content.

MATERIALS AND METHODS

Yeast Strains and Culture

Saccharomyces cerevisiae KNU5377 and ATCC24858 were used as described in the previous study [14]. *S. cerevisiae* KNU5377 was isolated from a sewage soil and characterized as a highly thermotolerant yeast [6]. The reference strain, *S. cerevisiae* ATCC24858, was originally reported in American Type Culture Collection as an ethanol-tolerant yeast and revealed as a moderately thermotolerant strain. When evaluated prior to this study, this reference strain showed high enough capacity to endure the thermal stress condition used in this study. However, general laboratory yeast strains, including *S. cerevisiae* W303, were found to be not useful as the reference because of their low thermotolerance level (unpublished). Both cells were grown with aeration to mid-exponential phase on YPD (1% yeast extract, 2% peptone 2%, 2% glucose) media at 30°C (10^6 – 10^7 cells/ml). In order to prepare heat-shocked cells for DSC (differential scanning calorimetry) analysis and cell-killing kinetic assay, mid-exponential cells were transferred to fresh YPD medium and subjected to a temperature shift to 43°C for 90 min, which induces maximum trehalose content in both strains.

Hyperthermic Cell-Killing Kinetics

The exponentially growing cells were incubated at 43°C, 48°C, 53°C, and 58°C, respectively, and aliquots were sampled at preset intervals. Aliquots were diluted with distilled water and adjusted to 100–200 colonies per plate. After overnight incubation of the plates at 30°C, cells were counted to determine the viabilities as colony-forming units (CFU/ml). Survival fraction, S , was determined as the percentage of cell numbers survived. Plots of $\ln S$ vs. incubation time provided the cell-killing rate constants. According to the critical target model, rate constants for cell killing are equivalent to denaturation rate constants of critical targets. Thus, the Arrhenius plots for the rate constants provide the Arrhenius parameters of the critical denaturation, as described previously [12].

Whole-Cell DSC Analysis

Cultures were harvested and washed twice with distilled water. The cell concentration was adjusted to 10^9 cells/ml. The cell suspension (1.2 ml) was injected into the sample cell of an MC-2 micro-calorimeter (Microcal Inc., Northampton, MA, U.S.A.). After a degassing process, the sample was subjected to DSC scans from 5°C to 100°C at a rate of 1°C/min. Distilled water was used as a reference. Both the

sample and reference were equilibrated at 5°C and heated to 100°C (1st scan). When the temperature was elevated to 100°C, they were rapidly cooled, equilibrated, and then heated again from 5°C to 100°C (2nd scan). After the first and second scans, DSC profiles of the second scanning was subtracted from the results of the first scanning. The remaining baseline curvature was adjusted by generating a cubic polynomial baseline to give corrected profiles. The endothermic profiles provided the C_p values (calorie/°C), representing the amounts of heat capacity during the denaturation of macromolecules. These measurements and data processing were conducted as previously described [13]. Critical denaturation profiles were predicted using the equation derived from the critical target model as

$$C_p = \frac{a}{v} \exp \left\{ A - \frac{E}{RT} - \frac{1}{v} \int_{T_i}^T \exp \left(A - \frac{E}{RT} \right) dT \right\}$$

where T_i , C_p , α , and v denote initial temperature of DSC scan, excess heat capacity of the denaturation, factor relating peak area to C_p , and rate of the temperature rise,

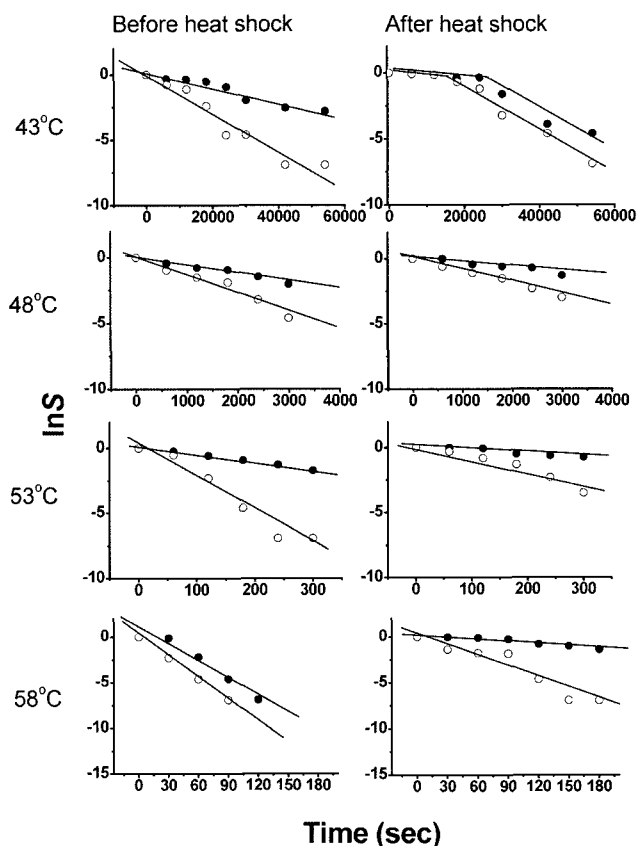


Fig. 1. Hyperthermic cell-killing profiles. Time-courses of $\ln S$ during incubation at 43, 48, 53, and 58°C are plotted with closed circles and open circles for KNU5377 and ATCC24858, respectively. Linear regression provided the solid lines.

respectively. The Arrhenius parameters E and $\exp(A)$ denote activation energy and frequency coefficient of critical denaturation in yeast cells, respectively.

RESULTS

Intrinsic Thermotolerance and the Stability of Cellular Components in *Saccharomyces cerevisiae* KNU5377

Cell-killing profiles at 43°C, 48°C, 53°C, and 58°C were examined for *S. cerevisiae* KNU5377 and *S. cerevisiae* ATCC24858 in mid-log phase (Fig. 1, before heat shock). All of them were monophasic, implying that a cell dies when one unit of target is irreversibly damaged. Linear fitting of the profiles provided the denaturation rate constant of critical targets. At all temperatures examined, *S. cerevisiae* KNU5377 was killed more slowly than *S. cerevisiae* ATCC24858, implying that *S. cerevisiae* KNU5377 is constitutively more thermotolerant than *S.*

Table 1. Arrhenius parameters for the critical endotherms.

Critical target denaturation	A	E (J/mol)
KNU5377		
Before HS [‡]	84.56	29013.77
After HS [‡]	33.39	12672.11
ATCC248458		
Before HS [‡]	77.07	26308.10
After HS [‡]	62.96	21901.75

The parameters for cell killing were determined by linear fitting of the Arrhenius plots (Fig. 1).

[‡]HS; Heat shock at 43°C for 90 min.

cerevisiae ATCC24858. The Arrhenius plots (Fig. 2) for the hyperthermic cell killing provided the Arrhenius parameters (Table 1), and critical endotherms were predicted from these parameters, E and A (Fig. 3). The critical endotherms showed that the critical target in *S. cerevisiae* KNU5377 was more stable by 3°C than that in the control (Fig. 3) with respect to the peak temperature (T_m) of the critical endotherm (Table 2).

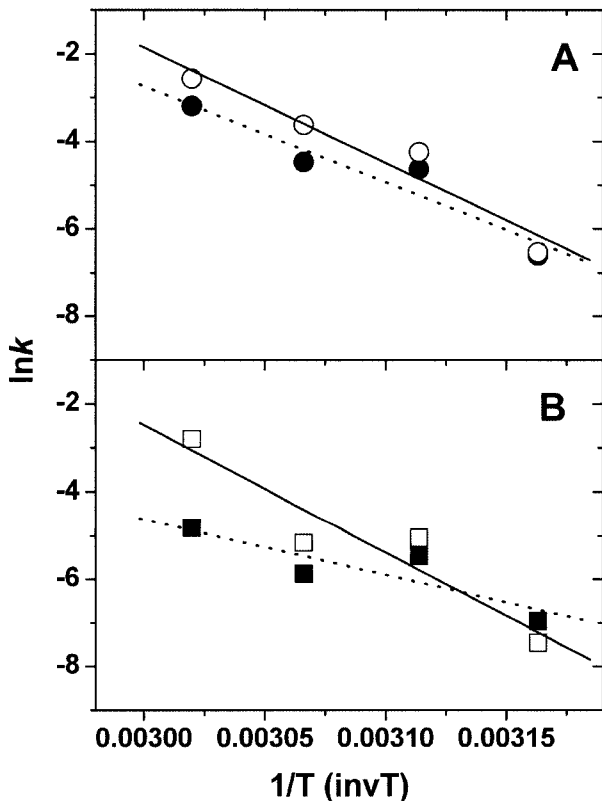


Fig. 2. Arrhenius plots of the rate constants for cell killing. Linear regression of the survival profiles in Fig. 1 gave apparent rate constants of cell killing in exponentially growing phase, and the logarithmic values before and after heat shock were plotted with open and closed symbols, respectively. Linear regression of the open and closed symbols gave the solid and dotted lines. Circles in panel A denote ATCC 24858 cells before (○) and after (●) heat shock in the exponentially growing phase, squares in panel B denote KNU5377 cells before (□) and after (■) heat shock.

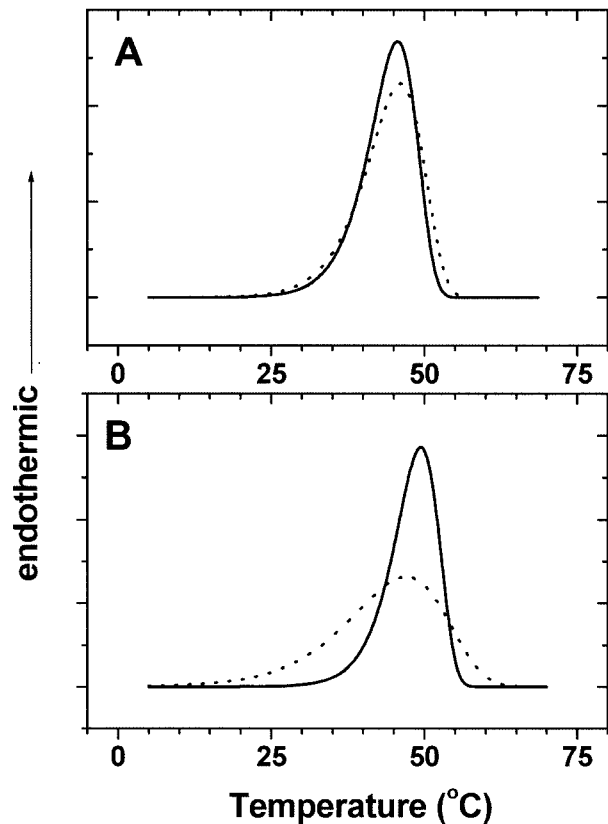


Fig. 3. Predicted critical endotherms before and after heat shock. The critical endotherms were predicted from the Arrhenius parameters (Table 1) resulted from Fig. 2. Panel A shows the critical endotherms of *S. cerevisiae* ATCC24858 strain, and panel B is *S. cerevisiae* KNU5377 strain. In both panels A and B, the solid, dashed, and dotted lines denote the critical endotherm before and after heat shock for 90 min, respectively.

Table 2. T_m values of irreversible transitions in whole-cell DSC profiles and predicted critical targets.

Transition profile	Before HS [‡]	After HS	Shift
Prominent transition*			
KNU5377**	59.9	60.7	+0.8°C
ATCC24858**	59.9	61.0	+1.1°C
Minor transition*			
KNU5377	47.9	50.0	+2.1°C
ATCC24858	49.1	51.1	+2.0°C
Critical target transition [†]			
KNU5377	49.1	47.0	-2.1°C
ATCC24858	45.8	46.1	+0.3°C

*Determined from the whole-cell DSC profiles.

†Determined from the critical denaturation profiles predicted by the critical target analysis.

***Saccharomyces cerevisiae* strains.

‡HS; Heat shock at 43°C for 90 min.

The whole-cell DSC profiles of both strains comprised a major transition and a minor transition that occurred before the major one (Fig. 4). The major transition occurred over the temperature range of 55 to 65°C in the whole-cell DSC profiles of both strains, and the peak temperatures, T_m , of both strains were identical (Table 2). The T_m of the minor transition in the profile of *S. cerevisiae* KNU5377 was lower by 1 than that of the control, but it did not show significant difference in overall patterns.

For *S. cerevisiae* KNU5377, the T_m of the minor transition was nearly the same as the predicted one for the critical denaturation (Table 2), and the temperature range of the minor transition included the range where the

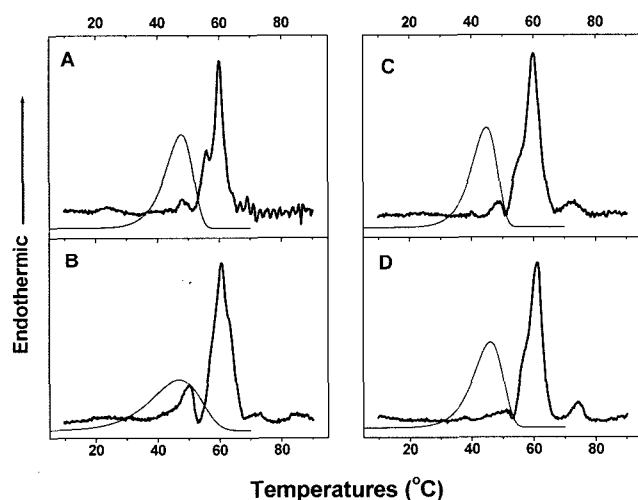


Fig. 4. Whole-cell DSC profiles and critical denaturation profiles. The profiles obtained by the DSC analysis are illustrated with thick lines. The critical denaturation profiles predicted by the critical target analysis are illustrated with thin lines. Left (A, B) and right (C, D) panels illustrate the profiles for KNU5377 and ATCC 24858, respectively. Upper (A, C) and lower (B, D) panels indicate before and after heat shock, respectively.

critical denaturation was predicted to occur (Fig. 4A). As shown in Fig. 4, the critical endotherm was magnified in order to localize it in whole-cell DSC profiles. The T_m of the minor transition was higher than that of the critical denaturation, and the temperature range where this minor transition occurred included the critical denaturation at the low-temperature edge of the minor transition. However, it should be noted that the critical targets of both strains were detected around the minor transitions.

Acquired Tolerance and the Stability of Cellular Components in *S. cerevisiae* KNU5377

Biphasic killing profiles were obtained at 43°C for the cells after heat shock, while monophasic profiles occurred at other temperatures examined (Fig. 1, after heat shock). The biphasic profiles comprised a shoulder phase where no killing occurred, followed by an exponentially killing phase. *S. cerevisiae* KNU5377 needed approximately 30,000 sec for the period of the shoulder, while the control strain, *S. cerevisiae* ATCC24858, needed about 10,000 sec. It is noted that the killing profiles of the cells before the heat shock were monophasic even at 43°C, suggesting that even this temperature was severe for them. However, the monophasic profiles changed by the heat shock into the exceptional profiles (i.e. biphasic profiles), implying that heat shock response altered the type of critical target.

At all temperatures examined, except at 43°C, the heat-shocked *S. cerevisiae* KNU5377 cells were killed at slower rates than the corresponding cells before the heat shock, showing that both strains acquired thermotolerance by their heat-shock responses (Fig. 1). However, even after the elevation of thermotolerance in *S. cerevisiae* ATCC24858, the intrinsic thermotolerance of *S. cerevisiae* KNU5377 exhibited higher thermotolerance than the acquired thermotolerance of the control strain, *S. cerevisiae* ATCC24858.

From the killing kinetics, the critical endotherms were predicted again (Figs. 2 and 3). The heat shock did not elevate the thermal stabilities of critical targets in both strains. The critical target of *S. cerevisiae* KNU5377 became labile after the heat shock, while the stability for the critical target of *S. cerevisiae* ATCC24858 was kept. Consequently, the difference by 3°C between both strains was reduced to approximately 1°C after the heat shock. However, even after the destabilization of critical targets by the heat shock, the critical target of *S. cerevisiae* KNU5377 was more stable than that of *S. cerevisiae* ATCC24858 (Table 2).

The whole-cell DSC profiles of both strains consisted of a prominent endothermic transition (i.e. major transition) and a preceding minor one (Fig. 4). The heat shock did not significantly change the T_m values of the prominent transition, but increased minor transitions by 2°C (Table 2).

DISCUSSION

The thermotolerance of *S. cerevisiae* KNU3577 in the mid-log phase was compared with that of the control strain, *S. cerevisiae* ATCC24858, and characterized using hyperthermic cell-killing kinetics and whole-cell DSC analyses.

The kinetic denaturation model gives the fitting equation for endothermic profiles that characterize irreversible thermal denaturation of biopolymers, and that the T_m of the endothermic profile characterizes the thermal stability of polymers [10]. In this work, the endothermic peaks of DSC profiles were classified with minor and major transitions; these transitions were arbitrarily named and classified with low (minor) and high (major) T_m values, respectively.

Cellular macromolecules or components in cells have their own denaturation range around their T_m values. Each denaturation profile of cellular components is put together into a mixed form in whole-cell DSC profiles. The variance of C_p values (Y axis) depends on the quantities of materials assayed, but it does not affect the T_m values. Therefore, the major transition in DSC profiles (Fig. 4) shows that most cellular components are denatured around the peak temperatures (T_m) of 60°C in both strains (Table 2). The minor transition appeared as a low height profile, implying that it includes relatively little amount of some cellular components that have denaturation temperatures different from the major transition. As for the intrinsic thermotolerance of *S. cerevisiae* KNU5377, the results indicate that there were no significant differences in the thermal stability of both strains, except that critical targets of both strains have different stability; the critical target of *S. cerevisiae* KNU5377 is 3°C higher than that of *S. cerevisiae* ATCC24858. The endotherms of critical targets, amplified in Fig. 4, were located around the minor transition in both strains. The minor transition can also include many cellular components; therefore, the localization of critical target might be embedded around the minor transition. This implies that it is difficult to identify by the DSC profiles which component in the minor transition is the critical target. However, it provides a clue for identifying the component by assaying fractionated cellular components. Although the whole-cell DSC profiles of both strains were not different from each other, it is also noted that the same kinds of cellular components in both strains may have different stability at an unseen state in the profiles. The intrinsic thermotolerance of *S. cerevisiae* KNU5377 would not be originated from the stability of entire components in cells, but probably from the stability of a critical target. This critical target is located around the minor transition that precedes the major one; therefore, it is highly likely that critical targets of both strains are relatively more thermolabile components than the major. However, the reason why the stability of critical target was different in both strains is not yet known. Fractionation study would be required for the answer.

On the other hand, the heat shock caused several changes in both strains: Firstly, it elevated thermotolerance in both strains. Secondly, the cell-killing rate decreased in both strains, except that of *S. cerevisiae* KNU5377 at 43°C. Thirdly, the minor transition was stabilized in both strains, showing similar DSC profiles pattern between both strains. Finally, the stability of the critical target of *S. cerevisiae* KNU5377 was reduced, but *S. cerevisiae* ATCC24858 maintained the stability.

As illustrated in Fig. 3, the exposure of *S. cerevisiae* KNU5377 cells to heat shock reduced the T_m value of the critical endotherm. The decrease resulted from an increase in rate constant for the first-order cell killing of the slope, following a shoulder at 43°C (Figs. 1 and 2). Even though the heat-shock exposure increased the cell-killing rate in KNU5377 at 43°C (Fig. 1), viabilities of the heat-shocked cells for longer than 30,000 sec were still higher than that of the non-heat-shocked cells (Fig. 1). Prior to the cell killing, there were shoulders in both strains where no killing occurred. Consequently, the heat-shock responses were responsible for the appearance of a shoulder, but it did not positively affect the cell-killing rate at 43°C in *S. cerevisiae* KNU5377. However, other temperature conditions, except 43°C, showed the first-order cell killing and reduced cell-killing rates, implying that the original properties of the target were changed by the heat shock at 43°C as a strain-specific phenomenon of *S. cerevisiae* KNU5377.

The biphasic profiles can be explained by the multiple-target model, which suggests that the single-target model works only under severe conditions [12]. It is noted that the killing profiles of the cells before the heat shock were monophasic even at 43°C, suggesting that even this temperature is severe for them. It can, therefore, be concluded that the heat-shock response altered the type of critical targets, and that it is a way of stabilization of strain KNU5377. However, the thermal stability of the critical target was still high in *S. cerevisiae* KNU5377 even after destabilization by the heat shock (Table 2), thus contributing higher thermotolerance (Fig. 1).

The heat-shock responses of both strains contributed to the stabilization of minor transition but not significantly to major transition (Table 2), and the whole-cell DSC profiles after the heat shock were also similar between both strains (Fig. 4). These results suggested that the heat-shock responses worked positively for the stabilizations of whole cells in both strains by similar actions, and that the main effect by the heat shock appeared to be enhanced stability of their minor transitions. This stabilization of cellular components has been suggested to be due to trehalose, because trehalose has been known as a disaccharide abundant *in vivo* after heat shock and an effective stabilizer of cellular components in yeast cells [16, 17]. *S. cerevisiae* KNU5377 has a much higher (2.6 times) concentration than the control strain, as reported previously [14]; however, the

trehalose content did not differ in the whole-cell DSC profiles of both strains.

In conclusion, the thermotolerant strain *S. cerevisiae* KNU5377 was characterized on its intrinsic thermotolerance as having both a higher stability of critical target and no relationship with the thermal stability of entire cellular components. Furthermore, the critical targets of both strains were located within their minor transitions that included more thermolabile components than major transition. In view of the acquired thermotolerance of *S. cerevisiae* KNU5377, the stabilization of cellular components and critical targets was not correlated closely with the trehalose amount, and heat-shock responses in the heat-shocked cells gave stronger contribution to the thermal stability of minor transitions than that of major transitions. This study has prompted us to clarify the critical target after fractionation of the cellular components and to study other mechanisms underlying the intrinsic tolerance that should be the key factors for the extremely high tolerance against various stressors in *S. cerevisiae* KNU5377 [19].

Acknowledgments

This project was supported by a grant (J9819) from the Korea Research Foundation for the Korea-Japan Collaborative Research Program and also by a grant (1998N-BIO2-P-02) from the Ministry of Commerce, Industry and Energy in Korea.

REFERENCES

1. Attfeld, P. V. 1987. Trehalose accumulates in *Saccharomyces cerevisiae* during exposure to agents that induce heat shock response. *FEBS Lett.* **225**: 257–263.
2. Gross, C. and K. Watson. 1996. Heat shock protein synthesis and trehalose accumulation are not required for induced thermotolerance in depressed *Saccharomyces cerevisiae*. *Biochem. Biophys. Res. Comm.* **220**: 766–772.
3. Gross, C. and K. Watson: 1998. Application of mRNA differential display to investigate gene expression in thermotolerant cells of *Saccharomyces cerevisiae*. *Yeast* **14**: 431–432.
4. Hottiger, T., P. Schmutz, and A. Wiemken. 1987. Heat-induced accumulation and futile cycling of trehalose in *Saccharomyces cerevisiae*. *J. Bacteriol.* **169**: 5518–5522.
5. Iwahashi, H., K. Obuchi, S. Fujii, and Y. Komatsu. 1995. The correlative evidence suggesting that trehalose stabilizes membrane structure in the yeast *Saccharomyces cerevisiae*. *Cell. Mol. Biol.* **41**: 763–769.
6. Kim, J. W., I. N. Jin, and J. H. Seu. 1995. Isolation of *Saccharomyces cerevisiae* F 38-1 (renamed to KNU5377), a thermotolerant yeast for fuel alcohol production at elevated temperature. *Kor. J. Appl. Microbiol. Biotechnol.* **23**: 617–623.
7. Lepock, J. R. and J. Kruuv. 1992. Mechanisms of thermal cytotoxicity. In Gerner, E. W. and Cetas, C. T. (eds.). *Hyperthermic Oncology*. Vol. 2. Arizona Board of Regents, Tuscon, Arizona.
8. Lepock, J. R., H. E. A. Frey, M. Rodhal, and J. Kruuv. 1988. Thermal analysis of CHL V79 cells using differential scanning calorimetry: Implication for hyperthermic cell killing and the heat shock response. *J. Cell. Physiol.* **137**: 14–24.
9. Lindquist, S. 1986. The heat-shock response. *Annu. Rev. Biochem.* **55**: 1151–1191.
10. Miles, D. A., L. Knott, I. G. Sumner, and A. Bailey. 1998. Differences between the thermal stabilities of the three triple-helicle domains of type IX collagen. *J. Mol. Biol.* **27**: 135–144.
11. Nwaka, S. and H. Holzer. 1998. Molecular biology of trehalose and the trehalases in the yeast *Saccharomyces cerevisiae*. *Prog. Nucleic Acid Res. Mol. Biol.* **58**: 197–237.
12. Obuchi, K., H. Iwahashi, J. R. Lepock, and Y. Komatsu. 1998. Stabilization of two families of critical targets for hyperthermic cell killing and acquired thermotolerance of yeast cells. *Yeast* **14**: 1249–1255.
13. Obuchi, K., H. Iwahashi, J. R. Lepock, and Y. Komatsu. 2000. Calorimetric characterization of critical targets for killing and acquired thermotolerance in yeast. *Yeast* **16**: 111–119.
14. Paik, S. K., H. S. Yun, H. Y. Sohn, and I. Jin. 2003. Effects of trehalose accumulation on the intrinsic and acquired thermotolerance in a natural isolate *Saccharomyces cerevisiae* KNU5377. *J. Microbiol. Biotechnol.* **13**: 85–89.
15. Ribeiro, M. J. S., J. T. Silva, and A. D. Panek. 1994. Trehalose metabolism in *Saccharomyces cerevisiae* during heat shock. *Biochem. Biophys. Acta* **1200**: 139–147.
16. Singer, M. A. and S. Lindquist. 1998. Thermotolerance in *Saccharomyces cerevisiae*: The Yin and Yang of trehalose. *Trends Biotechnol.* **16**: 460–468.
17. Sola-Penna, M. and J. R. Meyer-Fernandes. 1998. Stabilization against thermal inactivation promoted by sugars on enzyme structure and function: Why is trehalose more effective than other sugars? *Arch. Biochem. Biophys.* **360**: 10–14.
18. Wiemken, A. 1990. Trehalose in Yeast, stress protectant rather than reserve carbohydrate. *Antonie Van Leeuwenhoek* **58**: 209–217.
19. Yun, H. S., S. K. Paik, I. S. Kim, I. Jin, and H. Y. Sohn. 2004. Direct evidence of intracellular alkalization in *Saccharomyces cerevisiae* KNU5377 exposed to inorganic sulfuric acid. *J. Microbiol. Biotechnol.* **14**: 243–249.